Int. J. Heat Mass Transfer. Vol. 36, No. 10, pp. 2707–2710, 1993
Printed in Great Britain

0017–9310/93 $6.00 + 0.00

Natural convection heat transfer and fluid flow in an enclosure cooled at the top and heated at the bottom with roughness elements

M. RUHUL AMIN
Department of Mechanical Engineering, Montana State University, Bozeman, MT 59717, U.S.A.

(*Received* 29 *April* 1992 *and in final form* 15 *September* 1992)

INTRODUCTION

NATURAL convection heat transfer in rectangular enclosures heated from below has been the subject of many studies in recent years. Practical applications of such configurations are in electronic equipment and fluid-filled thermal storage tanks. The natural convection flows in fluids heated from below are inherently unstable [1, 2]. The fluid remains stationary up to a critical value of the temperature difference. Past the critical value, the onset of the motion depends on a balance of the viscous, buoyant, pressure and inertia forces.

Most of the previous works in this area were focused on smooth-walled enclosures [2–7]. Due to surface corrugation or mounting of circuit chips, the walls of the enclosure could be considered rough. Amin [8] studied the effect of placing adiabatic roughness elements at the bottom of a vertical enclosure with opposing hot and cold vertical walls. He concluded that roughness elements reduce the heat transfer rate across the enclosure. In the present study, a periodic array of roughness elements is mounted on the bottom hot horizontal wall (T_H^*). The top horizontal wall is cooled (T_C^*) and the two vertical walls are maintained adiabatic. This geometry is shown in Fig. 1. The effects of the size of the roughness elements on heat transfer and fluid flow phenomenon in the enclosure are studied in this note.

FORMULATION AND NUMERICAL METHOD

In the present work it is assumed that the natural convection flow of the Newtonian fluid in the enclosure of interest is at steady-state, is two-dimensional, and is laminar. It is also assumed that the Boussinesq approximation is valid, that the fluid is a radiatively non-participating medium and that viscous dissipation and compressive work are negligibly small. The radiation heat transfer between the walls is not being considered in this study.

Based on the above modeling assumptions, the non-dimensional governing equations for the conservation of mass, momentum and energy are

$$\frac{\partial u}{\partial x}+\frac{\partial v}{\partial y}=0 \tag{1a}$$

$$u\frac{\partial u}{\partial x}+v\frac{\partial u}{\partial y}=-\frac{\partial P}{\partial x}+\frac{\partial^2 u}{\partial x^2}+\frac{\partial^2 u}{\partial y^2} \tag{1b}$$

$$u\frac{\partial v}{\partial x}+v\frac{\partial v}{\partial y}=-\frac{\partial P}{\partial y}+\frac{\partial^2 v}{\partial x^2}+\frac{\partial^2 v}{\partial y^2}+\frac{Ra_H}{Pr}T \tag{1c}$$

$$u\frac{\partial T}{\partial x}+v\frac{\partial T}{\partial y}=\frac{1}{Pr}\left[\frac{\partial^2 T}{\partial x^2}+\frac{\partial^2 T}{\partial y^2}\right] \tag{1d}$$

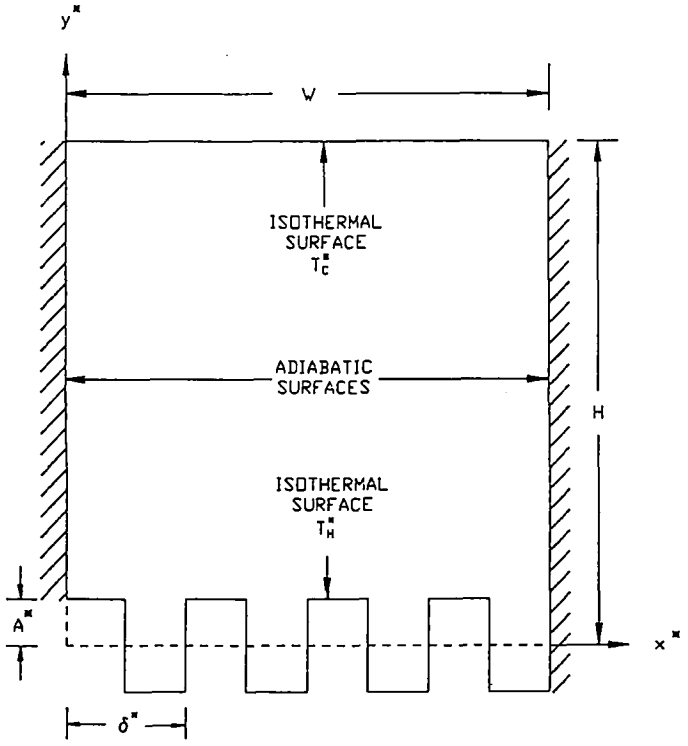

FIG. 1. Investigated geometry.

NOMENCLATURE

A^*	amplitude of roughness element, see Fig. 1
A	dimensionless amplitude of roughness element, A^*/H
C_p	constant pressure specific heat of fluid
g	magnitude of acceleration due to gravity
H	height of the enclosure
k	thermal conductivity of fluid
Nu	average Nusselt number of the enclosure, see equation (3)
P^*	motion pressure
P	dimensionless motion pressure, $P^*H^2/\rho\nu^2$
Pr	Prandtl number, $\mu C_p/k$
Ra_H	Rayleigh number, $g\beta\,(T_H^*-T_C^*)H^3/\nu\alpha$
T^*	temperature
T	dimensionless fluid temperature, $(T^*-T_C^*)/(T_H^*-T_C^*)$
T_H^*	hot wall temperature
T_C^*	cold wall temperature
u^*	x^*-component of velocity
u	dimensionless x-component of velocity, u^*H/ν
v^*	y^*-component of velocity
v	dimensionless y-component of velocity, v^*H/ν
W	width of enclosure
x^*, y^*	spatial coordinates, see Fig. 1
x, y	dimensionless spatial coordinates, $x^*/H, y^*/H$.

Greek symbols

α	thermal diffusivity of fluid
β	coefficient of thermal expansion of fluid
δ^*	period of roughness elements
δ	dimensionless period of roughness elements, δ^*/H
ε	tolerance parameter
μ	dynamic viscosity of fluid
ν	kinematic viscosity of fluid
ρ	density of fluid.

where P, the 'motion pressure' is defined as the actual pressure in the fluid less the pressure when the fluid is at rest at the reference temperature. The temperature of the cold vertical wall of the enclosure, T_C^*, serves as the reference temperature in the buoyancy force term in equation (1c).

The corresponding boundary conditions are described as follows:

$$u = v = 0, \quad \text{on all solid walls} \tag{2a}$$

$$\frac{\partial T}{\partial x} = 0, \quad \text{on the left vertical wall} \tag{2b}$$

$$T = 0, \quad \text{on the top horizontal wall} \tag{2c}$$

$$\frac{\partial T}{\partial x} = 0, \quad \text{on the right vertical wall} \tag{2d}$$

$$T = 1, \quad \text{on the bottom horizontal wall.} \tag{2e}$$

The overall heat transfer across the enclosure is expressed in terms of the average Nusselt number. The computation merely involves the integration of the local Nusselt number distribution along either the isothermal cold horizontal wall or the isothermal hot horizontal wall. For convenience, the cold wall is chosen for this purpose since it is always a plane surface, even in an enclosure containing roughness elements. The average Nusselt number in nondimensional form is defined as

$$Nu = \frac{1}{W/H}\int_0^{W/H} -\frac{\partial T(x,1)}{\partial y}\,dx. \tag{3}$$

The governing equations for the present study were solved by using the finite element code NACHOS II, developed by Gartling [9, 10]. This is a general purpose finite element code designed to solve the two-dimensional Navier–Stokes and energy equations for both steady-state and transient flows. A detailed description of the code has been documented elsewhere [9, 10], and will not be discussed here. Non-uniform grids were used such that more elements were packed into regions of large gradients of velocity and/or temperature.

For convergence criteria, NACHOS II uses the discrete norms defined by

$$d_{n+1}^U = \frac{1}{U_{\max}}\left[\sum_{i=1}^{N}(U_i^{n+1}-U_i^n)^2\right]^{1/2}$$

$$d_{n+1}^T = \frac{1}{T_{\max}}\left[\sum_{i=1}^{N}(T_i^{n+1}-T_i^n)^2\right]^{1/2}. \tag{4}$$

In equation (4), the subscript max indicates the maximum value of the variable found at the $(n+1)$th iteration, and N is the total number of nodal points. For convergence, the following inequalities were satisfied:

$$d_{n+1}^U \leqslant \varepsilon^U \quad \text{and} \quad d_{n+1}^T \leqslant \varepsilon^T \tag{5}$$

where ε, the tolerance parameter, was set to be 0.001.

RESULTS AND DISCUSSION

To check the accuracy of the NACHOS II code for the present problem, several cases were run at different values of Rayleigh number for a smooth-walled enclosure with aspect ratio $(W/H) = 1.0$. The computed values of the average Nusselt number for these cases were compared with the published results by Ozoe *et al.* [4]. This comparison is shown in Fig. 2. It can be seen that the results obtained by the present method are in good agreement with those of Ozoe *et al.* [4].

As discussed earlier, the natural convection flow of the present problem is inherently unstable. It was very difficult to obtain a stable solution at high values of Rayleigh numbers. Due to the limitation of the computer resources, the present study was conducted up to a maximum Rayleigh

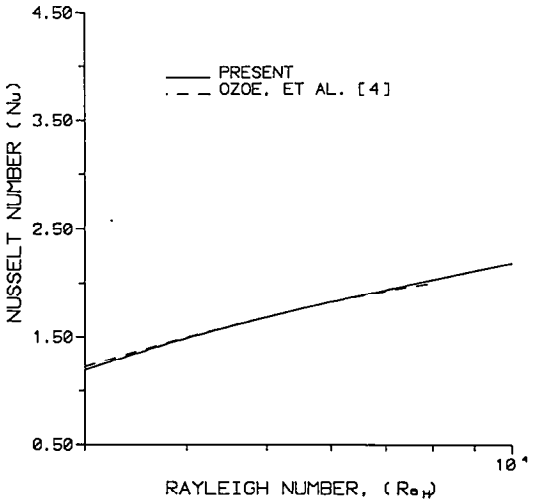

FIG. 2. Comparison of the results obtained by the present method with Ozoe *et al.* [4] for a smooth-walled enclosure.

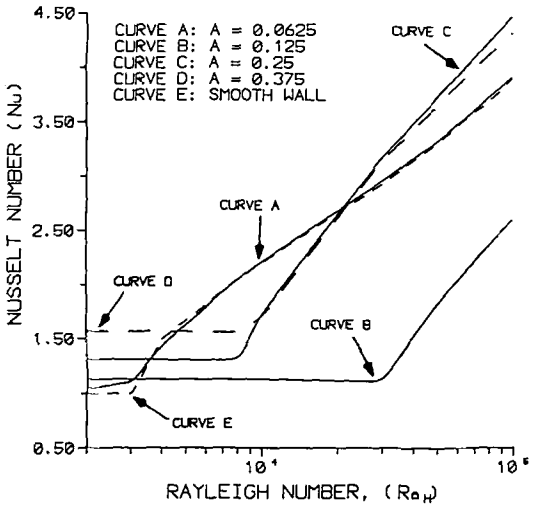

FIG. 3. Effect of amplitude on Nusselt number.

number of 10^5. A square enclosure (aspect ratio = 1.0) with a fluid of Prandtl number, $Pr = 10.0$, was used. The overall heat transfer rate and fluid flow phenomenon in the enclosure for various values of roughness element period and amplitude were investigated.

The results of this study show that in general, the presence of roughness elements on the hot horizontal wall increases the overall heat transfer rate across the enclosure in comparison with a corresponding smooth-walled enclosure. Figure 3 shows the effect of changing the amplitude (height) of roughness elements on the values of Nusselt number. It can be seen that at low values of Rayleigh number (conduction dominated flow), the Nusselt number increases with increase of roughness amplitude. This is as expected. The heat transfer across the enclosure is inversely proportional to the thermal resistance between the hot and cold walls. For conduction-dominated heat transfer, the thermal resistance is directly proportional to the distance between the hot and cold walls. So, increasing the amplitude decreases the effective distance between the walls and therefore, more heat transfer occurs.

Figure 3 also shows that in the range of Rayleigh numbers of approximately 4.5×10^3–1.8×10^4, heat transfer is more in a smooth-walled enclosure than that of a rough-walled enclosure. From the streamline and isotherm contours (not shown here due to space limitation) of the enclosures, it is observed that the presence of roughness elements delays the onset of convection motion. Therefore, heat transfer is more in the smooth-walled enclosure in this range. Beyond this range, the roughness elements increase the heat transfer rate across the enclosure except for cases with $A = 0.125$ (curve B), which will be discussed later. The heat transfer increases because the presence of roughness elements creates a stronger fluid motion inside the enclosure. This is verified by comparing the values of streamfunctions in the corresponding enclosures.

A very interesting feature occurred in this study. For smooth-walled enclosures ($A = 0$) the fluid flow inside the enclosure was confined to a single cell over the range of investigated Rayleigh numbers. As the amplitude, A, was gradually increased to 0.0625 and 0.1 (not shown in Fig. 3), the flow remained uni-cellular. The Nusselt numbers also remained close to the values of smooth-walled enclosures. This can be seen by comparing curve A and curve E in Fig. 3. However, when the amplitude was increased to a value of 0.125, the natural convection flow inside the enclosure became bi-cellular at a Rayleigh number of about 8×10^3. With a further increase of Rayleigh number for the same amplitude ($A = 0.125$), the flow with two cells eventually transformed to a flow with four cells at a Rayleigh number of about 3×10^4. In the range of Rayleigh numbers from 3×10^4 to 10^5, the flow remained quadru-cellular.

From the isotherm and streamline contours of the enclosure with $A = 0.125$, it is observed that the heat transfer rate is greatly reduced at higher values of Ra_H due to multicellular fluid motion inside the structure. Up to a value of $Ra_H = 3 \times 10^4$, the heat transfer across the enclosure remained conduction dominated. An example of fluid motion (streamlines) with four cells and the corresponding isotherms is shown in Fig. 4. It can be seen that the creation of four cells divides the entire enclosure into two regions along a horizontal axis of symmetry. The axis of symmetry is a little above the mid-height of the enclosure. The creation of these two opposing regions is the cause for such a drastic reduction of heat transfer in this particular geometry. Several cases for an enclosure with $A = 0.25$, were run to study the

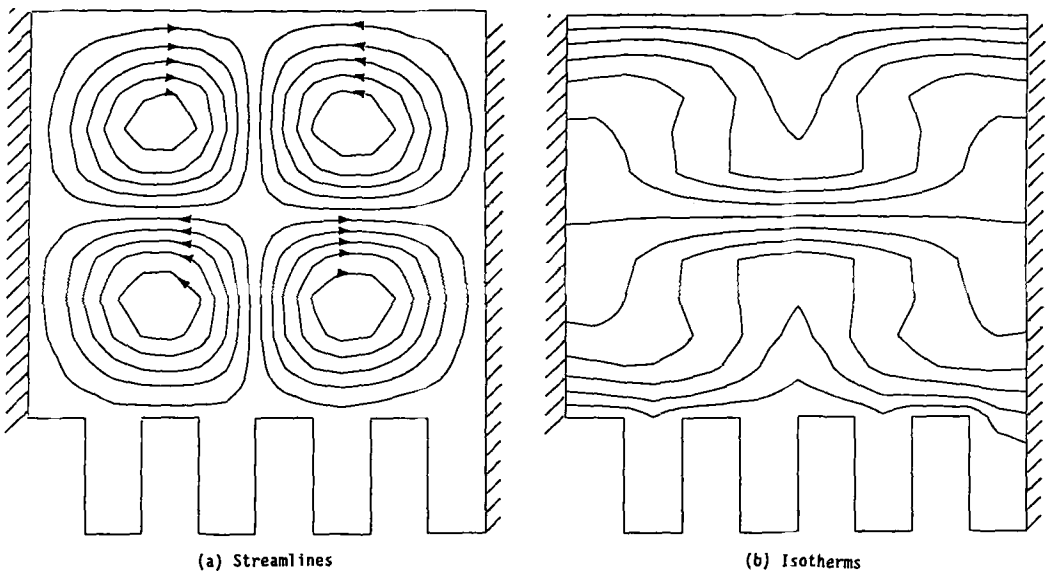

FIG. 4. Streamlines (a) and isotherms (b) for $Ra_H = 10^5$, $A = 0.125$, $\delta = 0.25$.

effect of changing the period, δ, from 0.25 to 0.5. A small decrement in heat transfer is observed in these cases. The maximum decrement obtained was about 4%.

In summary, the roughness elements are generally found to increase the heat transfer rate across the enclosure both at low and high Rayleigh numbers. The enhancement is more at low Rayleigh numbers in comparison with the cases with higher Rayleigh numbers. The maximum heat transfer enhancement (with respect to a corresponding smooth-walled enclosure) in this study is found to be 57%. This is obtained at $Ra_H = 2 \times 10^3$ for an enclosure with $A = 0.375$ and $\delta = 0.25$. In a transitional range between the conduction-dominated and convection-dominated cases, the presence of roughness elements delays the onset of convection motion. This effect reduces the heat transfer rate across the enclosure. For an enclosure with $A = 0.125$, the roughness elements generate a fluid motion with four cells at higher Rayleigh numbers. This effect drastically reduces the heat transfer rate across the enclosure. The maximum heat transfer decrement (with respect to a corresponding smooth-walled enclosure) in this geometry is found to be 61%, at a value of $Ra_H = 3 \times 10^4$.

REFERENCES

1. H. Ozoe and S. W. Churchill, Hydrodynamic stability and natural convection in Ostwald-de Waele and Ellis fluids: the development of a numerical solution, *A.I.Ch.E. Jl* **18,** 1196–1207 (1972).
2. M. R. Samuels and S. W. Churchill, Stability of a fluid in a rectangular region heated from below, *A.I.Ch.E. Jl* **13,** 77–85 (1967).
3. J. M. McDonough and I. Catton, A mixed finite difference Galerkin procedure for two-dimensional convection in a square box, *Int. J. Heat Mass Transfer* **25,** 1137–1146 (1982).
4. H. Ozoe, H. Sayama and S. W. Churchill, Natural convection in an inclined square channel, *Int. J. Heat Mass Transfer* **17,** 401–406 (1974).
5. H. Ozoe, K. Yamamoto, H. Sayama and S. W. Churchill, Natural circulation in an inclined rectangular channel heated on one side and cooled on the opposing side, *Int. J. Heat Mass Transfer* **17,** 1209–1217 (1974).
6. J. N. Arnold, I. Catton and D. K. Edwards, Experimental investigation of natural convection in inclined rectangular regions of differing aspect ratio, *J. Heat Transfer* **98,** 67–71 (1976).
7. I. Catton, P. S. Ayyaswamy and R. M. Clever, Natural convection flow in a finite, rectangular slot arbitrarily oriented with respect to the gravity vector, *Int. J. Heat Mass Transfer* **17,** 173–184 (1974).
8. M. R. Amin, The effect of adiabatic wall roughness elements on natural convection heat transfer in vertical enclosures, *Int. J. Heat Mass Transfer* **34,** 2691–2701 (1991).
9. D. K. Gartling, NACHOS II—A finite element computer program for incompressible flow problems, Part I—theoretical background, SAND86-1816, UC-32, Sandia Laboratories, Albuquerque, New Mexico (1987).
10. D. K. Gartling, NACHOS II—A finite element computer program for incompressible flow problems, Part II—user's manual, SAND86-1817, UC-32, Sandia Laboratories, Albuquerque, New Mexico (1987).

Int. J. Heat Mass Transfer. Vol. 36, No. 10, pp. 2710–2713, 1993
Printed in Great Britain

0017–9310/93 $6.00 + 0.00

Correlations for simultaneously developing laminar flow and heat transfer in a circular tube

B. SHOME and M. K. JENSEN†

Department of Mechanical Engineering, Aeronautical Engineering and Mechanics, Rensselaer Polytechnic Institute, Troy, NY 12180-3590, U.S.A.

(*Received* 7 *July* 1992 *and in final form* 9 *November* 1992)

INTRODUCTION

SIMULTANEOUSLY developing laminar flow and heat transfer in ducts has been widely analyzed in the past (see review by Shah and London [1]). More recent papers have shown that for accurate numerical solution of the classical Graetz problem (e.g. Conley *et al.* [2] and Poirier and Mujumdar [3]) or for simultaneously developing flow and heat transfer, Jensen [4], a very fine grid is needed to be concentrated at the tube inlet and wall where large gradients occur. Thus, most of the previous numerical studies are questionable at small non-dimensional distances because a variety of simplifications and coarse grids were used to obtain the solutions. Because the entrance length is significant for large Prandtl numbers ($Pr \geqslant 50$), accurate entrance length correlations for heat transfer and pressure drop are needed. However, very few correlations are available that can predict the local and/or average quantities. For example, the Churchill and Ozoe correlation [5], although covering the complete Pr and z^+ range, can predict only the local Nusselt number for the two limiting cases of constant wall temperature and constant wall heat flux, and its accuracy is known to degenerate for larger z^+ [1]. Therefore, the present investigation was initiated (i) to obtain accurate local and average Nusselt numbers for laminar flow through a straight circular tube with the general convective boundary condition, particularly very close to the entrance, and (ii) to develop accurate correlations for both local and average Nusselt numbers and friction factors, covering the complete Pr, Bi, and z^+ range.

† To whom any correspondence should be sent.

ANALYSIS

The non-dimensional governing equations for simultaneously developing laminar flow and heat transfer in a circular tube are:

$$\frac{1}{R}\frac{\partial}{\partial R}(RV_r) + \frac{\partial V_z}{\partial z^*} = 0 \tag{1}$$

$$V_r\frac{\partial V_z}{\partial R} + V_z\frac{\partial V_z}{\partial z^*} = -\frac{\partial P}{\partial z^*} + \frac{1}{R}\frac{\partial}{\partial R}\left(R\frac{\partial V_z}{\partial R}\right) \tag{2}$$

$$V_r\frac{\partial \Theta}{\partial R} + V_z\frac{\partial \Theta}{\partial z^*} = \frac{1}{Pr}\frac{1}{R}\frac{\partial}{\partial R}\left(R\frac{\partial \Theta}{\partial R}\right). \tag{3}$$